ChemElectroChem

Research Article
doi.org/10.1002/celc.202500190

Chemistry Europe
European Chemical Societies Publishing

www.chemelectrochem.org

Elucidating the Influence of Catalyst Cycling and Activation on the Activity of Ni-based Layered Double Hydroxides for Electrochemical Oxidation of Ethylene Glycol to Formate

Ina Kohlhaas and Regina Palkovits*

The efficient production of green hydrogen is a crucial step toward the development of economically effective ecological alternatives to fossil fuels. However, current water electrolysis still struggles with the high overpotential of the oxygen evolution reaction (OER). Replacing OER with electrochemical ethylene glycol oxidation (EGOR) would not only decrease the needed reaction potential for anode oxidation but also make use of the large amounts of polyethylene terephthalate (PET) waste produced every day. Ni-based layered double hydroxides (LDH) have previously found increased attention for their cost effectiveness, stability, and high catalytic activity in OER. This work discusses the applicability of Ni-based LDH materials in EGOR and investigates their catalytic ability in electrolysis, taking commonly used activation methods like cyclic voltammetry conditioning and chronoamperometric activation into account. The results confirm highly selective oxidation towards formate with yields of up to 30.7% for NiMn LDH and NiCo LDH at 1.4 V versus RHE, reaching Faraday efficiencies and carbon balances >90%.

1. Introduction

The intensive use of fossil fuel resources as a means to supply a majority of the energy needed has resulted in a massive rise in CO_2 emissions directly causing climate change and global warming.[1] Emission-free renewable energy sources like wind, water, or solar energy, while in theory economically competitive with fossil energy sources, currently only contribute to less than 10% of the global energy supply;[2,3] main reason being their daily and seasonal fluctuations resulting in an inconsistent energy supply. Implementing energy storage, for example, in form of hydrogen could easily circumvent this problem.[4,5] At present, most of our utilized hydrogen is still obtained from fossil fuels, however, it can be derived from electrochemical water splitting in an inexpensive, emission-free process.[5]

The main disadvantage of water electrolysis is the corresponding oxygen evolution reaction (OER) on the anode side of the electrolyser. With a thermodynamic potential of 1.23 V and an additional high overpotential, the sluggish kinetics of the OER present the limiting factor of the reaction lowering the reaction rate of hydrogen production and causing a high energy demand. Furthermore, the produced oxygen has little commercial value decreasing the overall economic feasibility of electrochemical water splitting.[6,7]

Plastic materials are indispensable in our modern everyday life as well as in industry. Post-consumer plastic waste currently accounts for 260 Mt of waste produced annually and corresponds to ≈2% of global CO_2 emission, numbers which are predicted to increase further in the next years.[2,8] Applying recycling methods, the materials can be regained and used again, decreasing not only the amount of waste but also the CO_2 production of plastic manufacturing.[1,8] Chemical recycling in particular is of high interest as polymers can be cleaved to regain access to their monomers. Polyethylene terephthalate (PET), for example, can be depolymerized by hydrolysis in alkaline media to obtain terephthalic acid (TA) and ethylene glycol (EG). Afterwards EG can undergo electrochemical conversion (electrochemical ethylene glycol oxidation, EGOR) toward formate/formic acid (jointly abbreviated as FA), which is a potential hydrogen carrier for energy storage and a valuable base chemical for industry.[1,9] Furthermore, the oxidation of EG can be coupled with hydrogen production at the cathode, leading to an alternative to electrochemical water splitting, optimizing both economic value and reaction efficiency.[6,10] Noble metal catalysts made from Pt, Pd, or Au document high activity in EGOR but are cost-intensive, vulnerable to poisoning and exhibit low selectivity, leading to a mix of C1 (FA, CO_2) and C2 products (glycolaldehyde, glycolate/glycolic acid (GA), oxalate/oxalic acid (OA)).[6,10–12] Non-precious transition metals are inexpensive and show high stability and activity under the respective reaction conditions. Recently numerous transition metal catalysts were reported to

I. Kohlhaas, R. Palkovits
Institute for Technical and Macromolecular Chemistry
RWTH Aachen University
Worringerweg 2, 52074 Aachen, Germany
E-mail: palkovits@itmc.rwth-aachen.de

R. Palkovits
Institute for a Sustainable Hydrogen Economy
Forschungszentrum Jülich
Marie-Curie-Str. 5, 52428 Jülich, Germany

Supporting information for this article is available on the WWW under https://doi.org/10.1002/celc.202500190

have high selectivity for EGOR toward FA.[10] Ni-based materials are cheap and abundant catalyst materials and among the best-performers for OER in alkaline water splitting. Due to its low-redox potential Ni is exceptionally well suited for reactions in alkaline solutions and has demonstrated promising activity in the formation of FA from EG.[1,10,13] Especially $Ni(OH)_2$ is commonly used either alone or in combination with other metals like Au nanoparticles achieving high FA selectivity >99% and good current densities above 100 mA cm^{-2}.[10,14]

Ni-based layered double hydroxides (LDH) are currently among the best-performers in alkaline water splitting making them interesting candidates for testing in alternative anode reactions to OER.[6,15–17] Combining Ni with a secondary metal that enables multiple oxidation states reportedly increases delocalization of charge within the hydroxide layer, facilitating OER by improving M—O bond cleavage (Scheme S1, Supporting Information).[18,19] In case of EGOR it was observed, that the favorable distribution of electron density was able to improve substrate adsorption on the catalyst surface and facilitate C—C bond cleavage (Scheme S2, Supporting Information).[20,21] Contrasting to pure hydroxide catalysts, the stabilization of the charge fluctuation is superior in LDH materials due to compensation of the increased positive charge by the interlayer anions.[18,19] Wang et al. published a method for direct formation of NiFe LDH on Ni foam enabling exceptional results for many anodic oxidation reactions, reporting EGOR toward FA at 99% conversion and 82% Faraday efficiency (FE) at initial current densities of up to 632 mA cm^{-2}.[22] In 2025 Ma et al. incorporated Mn into NiFe LDH, increasing the catalytic activity of the material, reaching FE values of up to 90% at 1.5 V versus RHE. Additionally, the group performed DFT calculations investigating the mechanism of EGOR on the LDH surface.[21] Despite these promising developments, Ni-based LDH materials are still often overlooked in EGOR research and insights on material optimization and structure activity relations remain rare.

In this article, we investigate the influence of the secondary metal on the electrocatalytic performance of Ni-based LDH materials in EGOR towards FA. The catalysts are characterized and examined regarding the influence of their composition on EGOR. The catalysts are subsequently tested in electrolysis evaluating the impact of electrode conditioning and activation on LDH materials.

2. Results and Discussion

NiMn, NiFe, and NiCo LDHs were synthesized with intercalated carbonate anions applying a co-precipitation method based on Berger et al.[15,23] Catalyst materials were characterized using XRD, IR spectroscopy, and ICP to check for LDH structure and material composition. All materials exhibit LDH characteristic reflexes at $2\theta = 12°$ (003), 23° (006), 35° (012), and 60° (110) (**Figure 1**), which can be attributed to the metals in the host layers. Intercalated anions are unlikely to be sufficiently organized to result in reflexes and usually hold low scattering intensity.[15,24–26] Additional reflexes observed for NiMn LDH can be attributed to unreacted $Mn(NO_3)_2$, which is generally not reported to have activity in electrochemical oxidation and therefore activity is assigned to formed LDH materials.[27,28] 2θ values of the (003) reflex are utilized to calculate the basal spacing of the LDH material using the Bragg equation. Reflexes appear at similar values of $2\theta = 11.60°$, 11.78° and 11.84° for NiMn, NiFe, and NiCo LDH, resulting in basal spacings of 7.62, 7.50, and 7.47 Å, respectively, indicating carbonate to be the interlayer anion in all synthesized catalysts. IR transmission spectroscopy (Figure S1, Supporting Information) was conducted to prove the intercalation of CO_3^{2-} as interlayer anion. The resulting signal at 1384 cm^{-1} can be attributed to CO_3^{2-} while the signal at 1645 cm^{-1} can be assigned to interlayer H_2O. ICP results confirm a Ni to secondary metal ratio of 0.45 for NiMn, 0.47 for NiFe and 0.51 for NiCo, respectively.

Afterwards, catalyst materials were coated onto a 1 × 1 cm Ni sheet and electrochemically characterized for OER and EGOR in 1 M KOH and 0.1 M EG in comparison to pure Ni. **Figure 2**a shows the obtained CVs without EG. For all synthesized LDH materials much lower onset potentials for OER compared to pure Ni are observed. However, while NiMn and NiCo perform similarly regarding the onset potential, NiFe exhibits a significantly lower onset potential of 1.42 V versus RHE in contrast to 1.50 V versus RHE obtained for NiMn and NiCo. Additionally, NiFe owns a much steeper increase in current density than the other tested

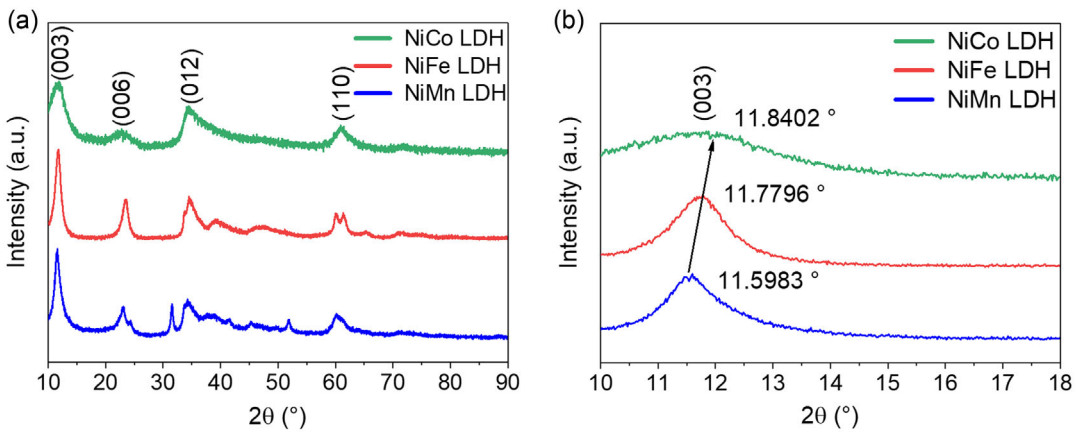

Figure 1. a) XRD of NiMn, NiFe, and NiCo LDH and b) position of (003) reflex of synthesized materials.

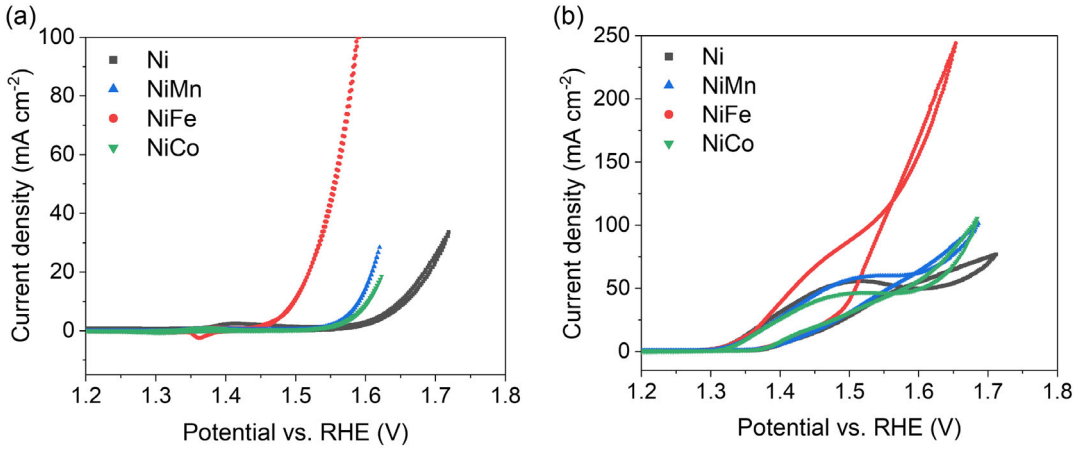

Figure 2. Cyclic voltammetry at 10 mV s^{-1} normalized to geometric area and 100% *iR* corrected a) in 1 M KOH and b) in 1 M KOH with 0.1 M EG.

materials. The superior activity of NiFe is in good agreement with literature regarding the OER activity of LDH materials.[16,29,30] Interestingly, literature presents no consistent results for the activity of NiMn and NiCo LDH.[29,30] Focusing on the CVs for the EGOR (Figure 2b), similar onset potentials of 1.28 V versus RHE can be noticed for all tested catalysts; the reason being that EG oxidation reportedly proceeds via a non-electrochemical follow-up reaction of the rate-determining electrochemical Ni^{2+}/Ni^{3+} oxidation, which has similar onset potentials for all tested materials during the CV in 1 M KOH without EG (Figure 2a).[14,31] In contrast, while still assumed the catalytically active species for OER, NiOOH formation during the Ni^{+2}/Ni^{3+} oxidation is not the potential limiting step in OER, increasing the onset potential compared to EGOR (Scheme S1 and S2, Supporting Information).[18,19,32] Comparing the material performance in EGOR, again NiFe possesses the highest catalytic activity whereas NiMn and NiCo both reach similar activities towards EGOR. Supporting the results of OER, both NiMn and NiCo outperform pure Ni after the start of competing OER at around 1.56 V versus RHE. The delayed onset of OER in presence of EG could origin from a higher reaction rate of EGOR at lower potentials inhibiting oxygen evolution.[31] Electrochemical impedance spectroscopy (EIS) results without EG (Figure S4a, Supporting Information) show charge transfer resistances (R_{ct}) of 0.89, 0.86, 0.33, and 1.04 Ω for Ni, NiMn, NiFe, and NiCo, respectively. As R_{ct} describes the electron transfer from the electrode into solution, it models the overall rate of the electrochemical reaction and should therefore be in line with other results describing the activity of the catalyst material.[33] However, in case of OER, results for R_{ct} do not follow activity trends observed in CV and therefore do not align with the expected trends. Based on CV results, it would have been predicted that Ni exhibits the highest R_{ct} of the tested materials while NiMn and NiCo were anticipated to perform similarly. All R_{ct} values rose when introducing EG into the system (Figure S4b, Supporting Information). NiFe provided the lowest increase of the measured samples yielding a R_{ct} value of 0.65 Ω, while NiMn exhibited the maximal value of 3.10 Ω. Ni and NiCo reached R_{ct} values of 2.52 and 3.03 Ω. Here, the results of EIS measurements again deviate from the expected trends based on CV, indicating that charge transfer is not the only influencing factor for catalyst activity. The double-layer capacitance (C_{dl}) (Figure S5 and S6, Supporting Information) was calculated based on the obtained current densities of CVs at different scan rates. CV values which had not reached a linear behavior in the area used to determine capacitive currents and outliers were excluded from C_{dl} calculation (and marked). This way, more precise trends for the overall behavior of the measurement could be achieved. Figure S5 and S6, Supporting Information indicate similar trends for both OER and EGOR. C_{dl} values grew in the order Ni < NiMn < NiCo < NiFe, reaching values of 35, 39, 48, and 50 μF cm^{-2} for OER and 37, 39, 42, and 43 μF cm^{-2} for EGOR, respectively. A possible explanation being the difference in particle size between the different LDH catalysts (Figure S2a, Supporting Information), leading to varying degrees of dispersion on the electrode surface and therefore varying C_{dl} values.

Electrolysis experiments oxidizing EG were performed for a duration of 2 h with and without additional conditioning or catalyst activation. For conditioning, CV cycles were recorded prior to electrolysis without EG between 1.2 and 1.5 V versus RHE covering the Ni^{2+}/Ni^{3+} oxidation and reduction peaks. For activation, 10 min of chronoamperometry (CA) without EG were conducted at a reaction potential of 1.4 V versus RHE to increase the number of active species on the electrode surface before EG oxidation. The product yield was normalized to C_{dl} of the catalyst on Ni foam (Figure S7, Supporting Information) to account for the variation in electrochemical surface area. Looking at the results of the electrolysis experiments (**Figure 3**a–c), the main product observed was FA with only small amounts of OA and negligible amounts of GA. Interestingly, in all cases the electrolysis results do not follow the trends of the CV studies (Figure 2) regarding catalyst performance. In results for electrolysis without pretreatment (Figure 3a), pure Ni foam exhibits the highest total yields of 24.9 ± 0.7% FA and 0.6 ± 0.6% OA. NiMn LDH on Ni foam presents the best outcome of the LDH materials of 19.6 ± 1.0% FA but still lower than pure Ni foam. NiCo LDH results in a slightly lower total yield of 18.2 ± 1.8% (17.1 ± 1.1% FA and 1.1 ± 0.7% OA), while NiFe LDH, the best-performer in CV measurements, only obtained a total yield of 9.6 ± 4.7% (9.4 ± 4.4% FA and 0.2 ± 0.3% OA). All catalysts, besides NiCo LDH (70.0 ± 0.5%),

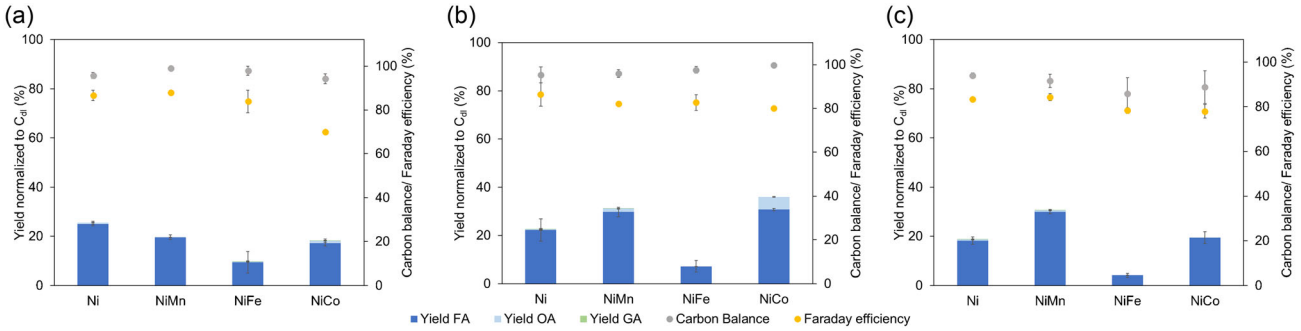

Figure 3. Electrolysis of 0.1 M EG in 1 M KOH a) without conditioning, b) with conditioning, and c) with activation. Electrolysis experiments were conducted for 2 h using Ni foam (CE) and Hg/HgO (RE).

show similar FE between 83.9 ± 5.2% (NiFe) and 87.8 ± 0.2% (NiMn) toward FA formation, which are comparable to literature.[21,22] All catalysts reached similar carbon balances (CB) of around 94.2 ± 2.3% (NiCo) to 98.9 ± 0.5% (NiMn). A decrease in FE while maintaining similar levels of CB and FA selectivity indicates elevated occurrence of OER as competing reaction to EGOR. C_{dl} trends on Ni foam (NiFe < Ni < NiCo < NiMn) (Figure S7, Supporting Information) and SEM images (Figure S2b, Supporting Information) suggest that NiMn and NiCo are more evenly deposited on the Ni foam than NiFe, therefore, leading to a higher active surface area, changing reactivity trends between CV and electrolysis results. Additionally, coated foam electrodes for electrolysis have a higher catalyst loading compared to the sheet electrodes used for CV studies. As LDH materials possess a lower conductivity in contrast to pure Ni, increasing the amount of catalyst would lessen the conductivity of the electrode and by comparison lead to better performance of pure Ni.[34] Furthermore, CA results (Figure S8a, Supporting Information) showcase that despite reaching initially higher current densities, matching CV results, the catalyst activity of NiFe shrank drastically over time, while the current densities of NiMn and NiCo improved. When conditioning the catalyst for 100 CV cycles without EG before electrolysis, no significant impact on pure Ni foam and NiFe LDH on Ni foam could be seen (Figure 3b). Yield, FE and CB stayed similar, however, the selectivity toward FA rose slightly compared to the reactions without any pretreatment and CA results confirm elevated catalyst stability over time (Figure S8b, Supporting Information).

In contrast, both NiMn and NiCo saw drastic enhancement in yield when conditioning before electrolysis (Figure 3b). In these cases, the FA yield improved by 10.1% and 13.6% from 19.6 ± 1.0% to 29.7 ± 2.0% (NiMn) and 17.1 ± 1.1% to 30.7 ± 0.47% (NiCo). Additionally, for both LDH materials the OA yield increased. While the CB and FE of NiMn kept the same, NiCo reveals a growth in FE, now reaching similar levels to the other catalysts, indicating less competing electrochemical reactions compared to the reaction without pretreatment. Commonly the effect of conditioning is explained by the transition of $Ni(OH)_2$ (Ni^{2+}) to NiOOH (Ni^{3+}). The amount of formed NiOOH is hereby depending on the oxidizability of the catalyst material.[35–37] In case of NiMn and NiCo, electrodes show a color change after pretreatment as well as a change in XRD reflexes (Figure S9, Supporting Information) and XPS energies (Figure S10a,c, Supporting Information), while NiFe measurements (Figure S9, Figure S10b, Supporting Information) retained more of the initial LDH structure, indicating a higher degree of oxidizability for NiMn and NiCo LDH. Literature reported the transformation of Ni forming a catalytically active hydrous NiO_xH_y layer with an anhydrous oxide layer underneath. It was observed that during conditioning the anhydrous oxide layer is partially reduced during cathodic sweeps facilitating a subsequent oxidation toward the hydrous NiO_xH_y species.[35,38,39] Furthermore, they saw a reduction of OER activity of Ni after conditioning and theorized an extended charge transport limitation from crystallinity of the formed NiO_xH_y layers canceling out the overall improved activity of the catalyst in some cases, which could explain the results observed for Ni and NiFe LDH.[35,40,41] The rise in activity for NiMn and NiCo after cycling, could be attributed to a possible additional oxidation of Mn and Co, which is reported to be advantageous for electrochemical oxidation, forming species that could act as additional active sites together with formed NiOOH.[42–46]

10 min of CA activation without EG at reaction potential was conducted to possibly stimulate the formation of Ni^{3+} from Ni^{2+}. CA activation results in a decreased performance of Ni and NiFe in comparison to no pretreatment and CV conditioning to 18.2 ± 1.5% for FA and 0.4 ± 0.2% for OA (Ni) 4.1 ± 0.8% for FA and 0% for OA (NiFe) while FE and CB stayed similar (Figure 3c). NiMn showed a growth in FA yield to 29.9 ± 2.4% compared to reactions without pretreatment and reached similar values to results with CV conditioning, while maintaining both FE and CB. The OA yield declined slightly to 0.8 ± 0.3% against results using CV conditioning. For NiCo (Yield FA: 19.5 ± 2.4%, OA: 0.7 ± 0.7%), no significant impact of CA activation as opposed to no pretreatment was observed and activity remained below the results with CV pretreatment. However, the OA yield dropped slightly. Additionally, the results illustrate an improved FE (81.6 ± 2.3%) to electrolysis experiments without pretreatment. All experiments confirm enhanced catalyst stability over the measurement duration compared to the base experiment (Figure S8c, Supporting Information). The difference in results between conditioning using 100 CV cycles (duration approx. 10 min) and activation at 1.4 V versus RHE for 10 min can indicate a difference in the number of active species formed. Results

support the assumption of Son et al. that Ni transforms, similarly to CV conditioning, into a catalytically active hydrous NiO_xH_y with an anhydrous oxide layer underneath. In contrast to CV conditioning CA activation is not able to reduce the anhydrous layer, therefore resulting in a thinner catalytically active layer.[35,47]

Overall, this study highlights the need to investigate electrocatalysts for EGOR not only in an as made state but also studying the impact of catalyst conditioning and activation to derive optimum candidates.

3. Conclusion

In this work, we investigated Ni-based LDH for application in EGOR. NiMn, NiFe and NiCo LDH were synthesized and electrochemical characterized using CV, EIS, and C_{dl}. Results confirm that Ni-based LDH materials are not only highly active OER catalysts but also promising candidates for EGOR, reaching high catalytic activity with onset potentials as low 1.28 V versus RHE. LDH materials were tested in electrolysis, investigating the impact of catalyst conditioning and activation on the materials. Results illustrate a growth in FA yield of up to 30.7% for NiMn and NiCo after conditioning, indicating the formation of highly active NiO_xH_y as well as a possible formation of oxidized Mn and Co species. In case of Ni and NiFe LDH, catalytic activity dropped after CV conditioning for 100 cycles between 1.3 and 1.6 V versus RHE, leading to the assumption of growing charge transfer limitation caused by increased crystallinity of NiO_xH_y which was previously reported in literature.[35,40,41] Catalyst activation via CA at 1.4 V versus RHE for 10 min led so similar results as CV conditioning but was not able to reach them completely. The observed results could be explained by the partial reduction of anhydrous NiO_xH_y layers during CV conditioning, which blocks further formation of active hydrous NiO_xH_y layers on the catalyst surface. This reduction is not possible during CA activation, leading to lower amounts of hydrous NiO_xH_y.[35,47]

4. Experimental Section

All chemicals and solvents are of analytical grade, commercially available and were used without further purification. Ni electrode materials were purchased from Goodfellow. Sodium carbonate (anhydrous), iron(III) nitrate nonahydrate, nickel(II) nitrate hexahydrate, and ethylene glycol were used from Merck. Cobalt(II) nitrate hexahydrate was bought from Roth and manganese(II) nitrate hexahydrate at abcr. Potassium hydroxide, ethanol and hydrochloric acid were available from Chemsolute. Nafion solution (5%) was purchased from Sigma Aldrich. All experiments were conducted using MilliQ water to prepare electrolyte solutions.

NiMn, NiFe, and NiCo were synthesized via co-precipitation similar to Berger et al.[15,23] 0.066 mol $Ni(NO_3)_2{\cdot}6H_2O$ and 0.033 mol of either $Fe(NO_3)_3{\cdot}9H_2O$, $Mn(NO_3)_2{\cdot}6H_2O$ or $Co(NO_3)_2{\cdot}6H_2O$ were dissolved in 40 mL of Milli Q water, in the following called solution A. Solution B was formed by dissolving 0.05 mol Na_2CO_3 in 100 mL Milli Q water. Solution A was added to solution B slowly under stirring to form the respective LDH material. Simultaneously, a 3.4 M NaOH solution was added dropwise to keep the pH value of the reaction solution at pH 10. The obtained suspension was stirred for 24 h at room temperature before filtrating and washing until the washing water turned pH 7. The solid was dried at 80 °C over night and ground in a ball milled at 50 rps for 5 min before use. X-ray diffraction patterns were collected using a Bruker D2 Phaser under CuK_α radiation ($\lambda = 1.54$ Å) with 1° incidence angle and 2θ ranging from 10° to 90° with 0.02° steps.

Electrochemical analysis of the materials was performed in a three-electrode cell with a Ni counter electrode (CE) and a Hg/HgO (1 M KOH) reference electrode (RE). The catalyst ink was prepared by mixing 5 mg of prepared LDH with 0.9 mL water and 0.9 mL ethanol and 10 μL Nafion solution (5%). The ink was sonicated for 30 min before use and drop casted on a 1 × 1 cm surface of a Ni sheet electrode 3 × 10 μL, resulting in a catalyst loading of 80 μg cm^{-2}. Ni electrodes were cleaned using 3 M HCl, acetone, isopropanol and MilliQ water before coating.

Ni foam electrodes for electrolysis were cleaned using 3 M HCl, acetone, isopropanol and MilliQ water. Working electrodes (WE) were pressed before use to mark a non-pressed 1 × 1 cm and coated with an ink made of 10 mg LDH, 0.9 mL water and 0.9 mL ethanol and 10 μL Nafion solution (5%), aiming for a catalyst coating of 3.5 mg cm^{-2}. The electrode was covered in Teflon tape, leaving the coated 1 × 1 cm surface area open. Electrolysis measurements were conducted in a three-electrode cell with a Ni foam CE and a Hg/HgO in 1 M KOH RE for 2 h at 1.4 V versus RHE in 1 M KOH with 0.1 M EG. During electrolysis measurements with conditioning, conditioning was performed prior to electrolysis as 100 CV cycles between 1.2 and 1.5 V versus RHE at 100 mV s^{-1} in 1 M KOH without EG. Catalyst activation during electrolysis with activation consisted of 30 min chronoamperometry at 1.4 V versus RHE in 1 M KOH without EG. The results were analyzed using HPLC.

Acknowledgements

This work was funded by the Federal Ministry of Research, Technology, and Space within Hydrogen Cluster4Future (HylnnoSep2 - FKZ: 03ZU2115EA) as well as the Cluster of Excellence Fuel Science Center (EXC 2186, ID: 390919832) funded by the Excellence Initiative by the German federal and state governments to promote science and research at German universities and the Japanese Society for the Promotion of Science (JSPS Postdoctoral Fellowship for Research in Japan (Short-term)). Support from German Research Foundation (DFG) within the project IRTG 2983 Hy-Potential (ID: 516338899) is gratefully acknowledged. The authors also acknowledge support of the Werner Siemens Foundation in the frame of the WSS Research Centre catalaix. We thank Nick Hausen and Matthias Urban for their help and input regarding XPS analysis.

Conflict of Interest

The authors declare no conflict of interest.

Data Availability Statement

The data that support the findings of this study are available from the corresponding author upon reasonable request.

Keywords: electrochemistry · electrochemical ethylene glycol oxidation · electrosynthesis · hydrogen

[1] I. Bashir, J. D. McGettrick, M. F. Kühnel, B. Sarfraz, S. N. Arshad, A. Rauf, *ACS Sustainable Chem. Eng.* **2024**, 4795.
[2] Y. Ma, Y. Zhang, W. Yuan, M. Du, S. Kang, B. Qiu, *EES Catal.* **2023**, *1*, 892.
[3] S. R. Sinsel, R. L. Riemke, V. H. Hoffmann, *Renewable Energy* **2020**, *145*, 2271.
[4] S. Ould Amrouche, D. Rekioua, T. Rekioua, S. Bacha, *Int. J. Hydrogen Energy* **2016**, *41*, 20914.
[5] S. Shiva Kumar, H. Lim, *Energy Rep.* **2022**, *8*, 13793.
[6] X. Lu, Y. Guo, H. Fu, J. Song, C. Liang, H. Jiang, Z. Wang, Y. Liu, H. Cheng, Z. Zheng, Y. Wu, P. Wang, B. Huang, *Renew. Sust. Ener. Rev.* **2024**, *195*, 114333.
[7] S. C. Cho, J. H. Seok, H. N. Manh, J. H. Seol, C. H. Lee, S. U. Lee, *Nano Convergence* **2025**, *12*, 4.
[8] Z. Chen, W. Wei, X. Chen, Y. Liu, Y. Shen, B.-J. Ni, *Renewable Sustainable Energy Rev.* **2024**, *195*, 114333.
[9] M. Du, Y. Zhang, S. Kang, C. Xu, Y. Ma, L. Cai, Y. Zhu, Y. Chai, B. Qiu, *Small* **2023**, *19*, e2303693.
[10] K. Liu, Y. Wang, F. Liu, C. Liu, R. Shi, Y. Chen, *Chem. Eng. J.* **2023**, *473*, 145292.
[11] X. Zhang, R. Wei, M. Yan, X. Wang, X. Wei, Y. Wang, L. Wang, J. Zhang, S. Yin, *Adv. Funct. Mater.* **2024**, *34*, 2401796.
[12] Y. Wang, K. Liu, F. Liu, C. Liu, R. Shi, Y. Chen, *Green Chem.* **2023**, *25*, 5872.
[13] J. Li, L. Li, X. Ma, X. Han, C. Xing, X. Qi, R. He, J. Arbiol, H. Pan, J. Zhao, J. Deng, Y. Zhang, Y. Yang, A. Cabot, *Adv. Sci.* **2023**, *10*, e2300841.
[14] D. Du, F. Kang, S. Yang, B. Shao, J. Luo, *Sci. China Chem.* **2024**, *67*, 1539.
[15] M. Berger, I. M. Popa, L. Negahdar, S. Palkovits, B. Kaufmann, M. Pilaski, H. Hoster, R. Palkovits, *ChemElectroChem* **2023**, *10*, e202300235.
[16] P. M. Bodhankar, P. B. Sarawade, G. Singh, A. Vinu, D. S. Dhawale, *J. Mater. Chem. A* **2021**, *9*, 3180.
[17] D. Chaillot, S. Bennici, J. Brendlé, *Environ. Sci. Pollut. Res. Int.* **2021**, *28*, 24375.
[18] J. Mohammed-Ibrahim, *J. Power Sources* **2020**, *448*, 227375.
[19] S. Anantharaj, K. Karthick, S. Kundu, *Mater. Today Energy* **2017**, *6*, 1.
[20] J.-J. Zhao, H.-R. Zhu, C.-J. Huang, M.-H. Yin, G.-R. Li, *J. Mater. Chem. A* **2025**, *13*, 3236.
[21] Y. Ma, H. Ge, Y. Zhang, N. Jian, J. Yu, J. Arbiol, C. Li, Y. Zhong, L. Li, H. Kang, J. Wang, A. Cabot, J. Li, *ACS Sustainable Chem. Eng.* **2025**, *13*, 5601.
[22] C. Wang, Y. Wu, A. Bodach, M. L. Krebs, W. Schuhmann, F. Schüth, *Angew. Chem. Int. Ed.* **2023**, *62*, e202215804.
[23] M. Berger, A. Markus, S. Palkovits, R. Palkovits, *ChemElectroChem* **2024**, *11*, e202400457.
[24] S. A. de Waal, E. A. Viljoen, *Am. Mineral.* **1971**, *56*, 1077.
[25] A. Flegler, S. Müssig, J. Prieschl, K. Mandel, G. Sextl, *Electrochim. Acta* **2017**, *231*, 216.
[26] A. Flegler, M. Schneider, J. Prieschl, R. Stevens, T. Vinnay, K. Mandel, *RSC Adv.* **2016**, *6*, 57236.
[27] G. A. Tikhomirov, K. O. Znamenkov, I. V. Morozov, E. Kemnitz, S. I. Troyanov, *Z. Anorg. Allg. Chem.* **2002**, *628*, 269.
[28] M. Li, D. Ma, X. Feng, C. Zhi, Y. Jia, J. Zhang, Y. Zhang, Y. Chen, J.-W. Le Shi, *Small* **2025**, *21*, e2412576.
[29] F. Dionigi, J. Zhu, Z. Zeng, T. Merzdorf, H. Sarodnik, M. Gliech, L. Pan, W.-X. Li, J. Greeley, P. Strasser, *Angew. Chem.* **2021**, *133*, 14567.
[30] O. Diaz-Morales, I. Ledezma-Yanez, M. T. M. Koper, F. Calle-Vallejo, *ACS Catal.* **2015**, *5*, 5380.
[31] W. Chen, J. Shi, C. Xie, W. Zhou, L. Xu, Y. Li, Y. Wu, B. Wu, Y.-C. Huang, B. Zhou, M. Yang, J. Liu, C.-L. Dong, T. Wang, Y. Zou, S. Wang, *Nat. Sci. Rev.* **2023**, *10*, nwad099.
[32] F. Dionigi, Z. Zeng, I. Sinev, T. Merzdorf, S. Deshpande, M. B. Lopez, S. Kunze, I. Zegkinoglou, H. Sarodnik, D. Fan, A. Bergmann, J. Drnec, J. F. de Araujo, M. Gliech, D. Teschner, J. Zhu, W.-X. Li, J. Greeley, B. R. Cuenya, P. Strasser, *Nat. Commun.* **2020**, *11*, 2522.
[33] D. Li, H. Liu, L. Feng, *Energy Fuels* **2020**, *34*, 13491.
[34] H. Wang, B. Yang, R. L. Smith, Y. Su, X. Qi, *Adv. Funct. Mater.* **2025**, *35*, 2425333.
[35] Y. J. Son, S. Kim, V. Leung, K. Kawashima, J. Noh, K. Kim, R. A. Marquez, O. A. Carrasco-Jaim, L. A. Smith, H. Celio, D. J. Milliron, B. A. Korgel, C. B. Mullins, *ACS Catal.* **2022**, *12*, 10384.
[36] A. Sivanantham, P. Ganesan, A. Vinu, S. Shanmugam, *ACS Catal.* **2020**, *10*, 463.
[37] J. Masa, W. Schuhmann, *ChemCatChem* **2019**, *11*, 5842.
[38] M. E. G. Lyons, R. L. Doyle, I. Godwin, M. O'Brien, L. Russell, *J. Electrochem. Soc.* **2012**, *159*, H932.
[39] L. D. Burke, E. J. O'Sullivan, *J. Electroanal. Chem. Interfacial Electrochem.* **1981**, *117*, 155.
[40] M. E. Lyons, A. Cakara, P. O'Brien, I. Godwin, R. L. Doyle, *Int. J. Electrochem. Sci.* **2012**, *7*, 11768.
[41] M. E. Lyons, L. Russell, M. O'Brien, R. L. Doyle, I. Godwin, M. P. Brandon, *Int. J. Electrochem. Sci.* **2012**, *7*, 2710.
[42] N. Arjona, F. Espinosa-Magaña, J. A. Bañuelos, L. Álvarez-Contreras, M. Guerra-Balcázar, *ChemElectroChem* **2022**, *9*, e202200015.
[43] Z. Fang, X. Du, K. Qian, Z. Deng, A. Hong, T. Li, T. Wei, R. Li, *Int. J. Hydrogen Energy* **2024**, *74*, 39.
[44] Y. Wang, J. Liu, H. Yuan, F. Liu, T. Hu, B. Yang, *Adv. Funct. Mater.* **2023**, *33*, 2211909.
[45] B. Liu, C. Wu, C. Wen, H. Li, Y. Shimura, H. Tatsuoka, B. Sa, *Electrochim. Acta* **2022**, *408*, 139965.
[46] T. Zhang, S. Zhao, C. Zhu, J. Shi, C. Su, J. Yang, M. Wang, J. Li, J. Li, P. Liu, C. Wang, *Nano Res.* **2023**, *16*, 624.
[47] R. L. Doyle, I. J. Godwin, M. P. Brandon, M. E. G. Lyons, *Phys. Chem. Chem. Phys.* **2013**, *15*, 13737.

Manuscript received: May 13, 2025
Revised manuscript received: June 16, 2025
Version of record online: